FRACTIONAL PREDICTION OF GROUND TEMPERATURE BASED ON SOIL FIELD SPECTRUM

by

An-Hong TIAN[a], Hei-Gang XIONG[b*], Cheng-Biao FU[a*], Zheng-Biao LI[c], and Long YU[d]

[a] College of Information Engineering, Qujing Normal University, Qujing, China
[b] College of Applied Arts and Science, Beijing Union University, Beijing, China
[c] Department of Science and Technology, Qujing Normal University, Qujing, China
[d] School of City, Qujing Normal University, Qujing,China

Original scientific paper
https://doi.org/10.2298/TSCI2004301T

Ground temperature is an important physical indicator reflecting the natural ecological environment of the Earth's surface. Soil spectrum is a comprehensive reflection of soil properties, but there are few studies on the prediction of ground temperature based on soil field spectrum using fractional calculus. In this paper, the fractional derivative is used to study the correlation between soil spectrum and ground temperature from zeroth order to second order, and the characteristic wavelength bands are extracted. Simulations show that the fractional approach can amplify the difference of the soil field spectral signal. The wavelength bands for the 0.01 significance test begin with 0.6^{th} order, while the 1.3^{th} order sees 33 wavelength bands. Coefficients of determination of 0.7, 0.8, 0.9, 1.3, 1.4, 1.5, 1.6, and 1.7-order are all greater than 0.66, indicating that the established model of linear stepwise multiple regression gives a better prediction.

Key words: *ground temperature, fractional derivate, soil field spectra signal, model evaluation criteria*

Introduction

Ground temperature is an important physical parameter of the interaction process of the Earth air system [1, 2]. It is also an important physical indicator reflecting the natural ecological environment of the Earth's surface. It is widely used in the research of surface radiant energy balance, soil moisture estimation, urban heat island effect monitoring, and remote sensing drought index [3, 4]. The traditional ground temperature acquisition method mainly relies on human measurement, but due to various reasons such as equipment and manpower, the measurement range is very limited [5, 6]. However, the characteristics of all-weather, multi-temporal, and large-scale hyperspectral remote sensing data provide an effective means for obtaining ground temperature data [7, 8].

Because the soil hyperspectral signal contains more than 2000 bands, there are many problems such as huge data volume, numerous collinear bands and serious information redundancy. Therefore, preprocessing of the original spectral signals is an important step in spectral modeling. Traditional calculus (including first-order and second-order calculus) is a commonly used spectral signal preprocessing method, however, this method only considers

* Corresponding author's, e-mail: xionghg2017@163.com, fucbfly@163.com

the first-order differential derivative or the second-order differential derivative of the spectral signal, ignoring the spectral reflectance characteristics of the fractional derivative, resulting in low modeling accuracy.

Due to the memory characteristics of fractional calculus, it can extract sensitive wavelength bands useful for predictive models, and it has been used in soil spectral signal analysis in recent years. For example, Xia *et al.* [9] used fractional derivative to study the relationship between indoor spectra and conductivity, simulation results showed that the fractional derivative could extract the detailed information of the soil spectral signal change. Wang *et al.* [10] used the fractional derivative to study the salt content of Ebinur Lake Wetland. The simulations showed that the prediction model based on the fractional 1.5-order random forest was optimal to estimate salt content. However, these studies are based on the analysis of indoor spectral characteristics. At present, there are little studies on the fractional derivatives used in the field spectrum. However, the field spectral acquisition is more consistent with the actual environmental conditions of the sampling point, and the satellite-borne hyperspectral remote sensing data acquisition is also the field spectrum, so the field spectral value is more explored. In this study, the field spectrum and ground temperature of Xinjiang were collected in May 2017, and the prediction result of ground temperature by hyperspectral remote sensing was studied to provide a theoretical reference value for agricultural management.

Materials and methods

Spectral characteristics of the ground object

There are three basic physical processes of the interaction between electromagnetic radiation and the Earth's surface, namely reflection, absorption, and transmission, this relationship can be described:

$$E(\lambda) = E_{\mathrm{R}}(\lambda) + E_{\mathrm{A}}(\lambda) + E_{\mathrm{T}}(\lambda) \tag{1}$$

where $E(\lambda)$ is the incident energy, $E_{\mathrm{R}}(\lambda)$ – the reflection energy, $E_{\mathrm{A}}(\lambda)$ – the absorption energy, and $E_{\mathrm{T}}(\lambda)$ – the transmission energy.

The object's surface thermal radiation is almost equal to zero in the bands of visible and near-infrared. The spectrum emitted by the ground objects is mainly based on the reflection of solar radiant energy. When electromagnetic radiation reaches the interface of two different media, the phenomenon that part or all of the incident energy returns to the original medium is called reflection. The characteristics of the reflection can be expressed in terms of reflectivity. Reflectivity, ρ, is the ratio of reflection energy to incident energy, it is a function of wavelength, also known as the spectral reflectance rate $\rho(\lambda)$, which is defined:

$$\rho(\lambda) = \frac{E_{\mathrm{R}}(\lambda)}{E(\lambda)} 100\% \tag{2}$$

Measurement field spectrum and ground temperature

The desert soil in Xinjiang's Fukang was selected as the study area, and the location information of 30 sampling points is shown in fig. 1. The field spectrum acquisition time was in May 2017. Field Spec® 3Hi-Res spectrometer was used to collect the surface spectrum of the sampling point, and the ground temperature of the sampling point was collected by a thermal infrared temperature instrument. In addition, since the field spectrum is disturbed by soil moisture, the moisture absorption bands around 1300 nm and 1900 nm need to be removed.

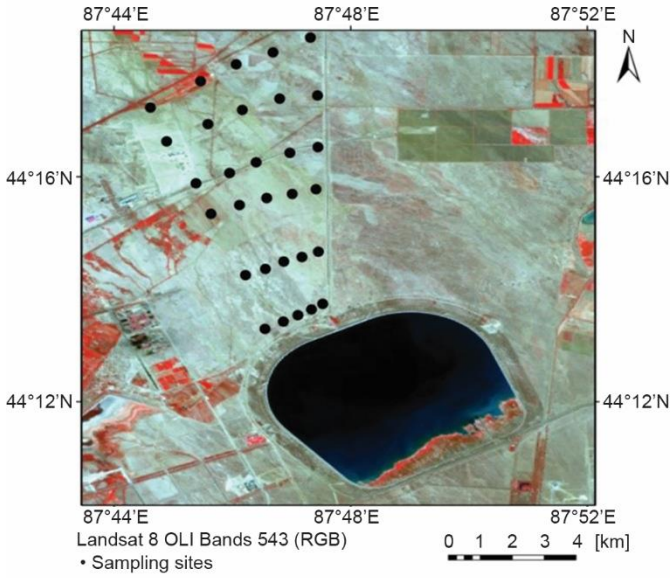

Figure 1. Soil sampling points location

Fractional-order derivate and correlation coefficient

The definition of Gruennwald-Letnikov fractional derivative [11] is defined:

$$ {}_a\mathrm{D}_b^{\beta} f(\mathrm{x}) = \lim_{h\to 0} \frac{1}{h^{\beta}} \sum_{r=0}^{[(b-a)/h]} (-1)^r \binom{\beta}{r} f(x-rh) \tag{3}$$

where β is the fractional order, a – the lower limit of the differential, b – the upper limit of the differential, h – the sampling interval, and $(\beta\ r)$ – a binomial coefficient:

$$ \binom{\beta}{r} = \begin{cases} 1 & , j = 0 \\ \dfrac{\Gamma(\beta+1)}{\Gamma(r+1)\Gamma(\beta-r+1)} & , j > 0 \end{cases} \tag{4}$$

where $\Gamma(.)$ is a gamma function:

$$ \Gamma(x) = \int_0^{+\infty} t^{x-1}\mathrm{e}^{-t}\mathrm{d}t \tag{5}$$

Since the sampling interval of the spectrometer is equal to 1, the differential expression of eq. (3) is:

$$ \frac{\mathrm{d}^v f(x)}{\mathrm{d}x^v} \approx f(x) + (-1)vf(x-1) + (-1)^2 \frac{(v)(v-1)}{2} f(x-2) + $$

$$ \ldots + (-1)^n \frac{\Gamma(v+1)}{n!\Gamma(v-n+1)} f(x-n) \tag{6}$$

where v is order, $n = [(b - a)/h]$.

In this paper, the Gruenwald-Letnikov fractional derivate values of soil spectrum have been calculated out within 0.1 fractional interval between 0.0-order and 2.0-order.

Model evaluation criteria

Coefficient of determination, R^2, and RMSE are used as criteria for judging the advantages of the model. The square of the correlation coefficient is equal to the R^2. When $0.66 \le R^2 \le 0.80$, the model fitting effect is better. When $0.81 \le R^2 \le 0.90$, the model fitting result is very good. When $R^2 \ge 0.90$, the model fits extremely excellently. The R^2 and RMSE are defined, respectively:

$$R^2 = \left[\frac{\sum_{i=1}^{n}(x_i - \bar{x})(y_i - \bar{y})}{\sqrt{\sum_{i=1}^{n}(x_i - \bar{x})^2 \sum_{i=1}^{n}(y_i - \bar{y})^2}} \right]^2 \tag{7}$$

$$RMSE = \sqrt{\frac{1}{N-1}\sum_{i=1}^{N}(y_i - \hat{y}_i)^2} \tag{8}$$

where x represents the soil spectral reflectance, y – the ground temperature value of the sampling point, $\bar{x}$ – the mean value of the soil spectral reflectance, and $\bar{y}$ – the mean value of the ground temperature of the sampling point, and $\hat{y}$ – the output value of the model.

Simulation results

Correlation coefficient between ground temperature and original spectra

According to eqs. (6) and (7), we can calculate the fractional correlation coefficient of ground temperature and soil spectral reflectance. Beginning with zeroth order with a fractional order interval of 0.1. The significance test was performed at the 0.01 level. The results are shown in fig. 2. Figure 2(a) shows that the correlation coefficients do not pass through the 0.01 significance level between 0.0-order and 0.5-order. Figures 2(b)-2(f) show that some wavelength bands passing through the 0.01 significance level are from the 0.6-order. Figure 2(b) shows that the wavelength bands of the 0.6-order passing through the 0.01 significance level range from 2150 nm to 2350 nm, and the 0.7-order ranges from 980 nm to 1000 nm, and from 2100 nm to 2310 nm. Figures 2(c)-2(f) show that the number of wavelength bands passing through the 0.01 significance level from the 0.8-order to 2.0-order are much more than those of 0.6-order and 0.7-order.

Significance wavelength bands number and max correlation coefficient under different fractional-order derivate

Significance bands number and max correlation coefficient under different fractional-order derivatives are given in tab. 1. It can be seen from tab. 1 that there are no wavelength bands with a significance test of 0.01 between 0.0-order and 0.5-order, the number of wavelength bands in 1.3-order is up to 33. The max correlation coefficient between 0.6-order and

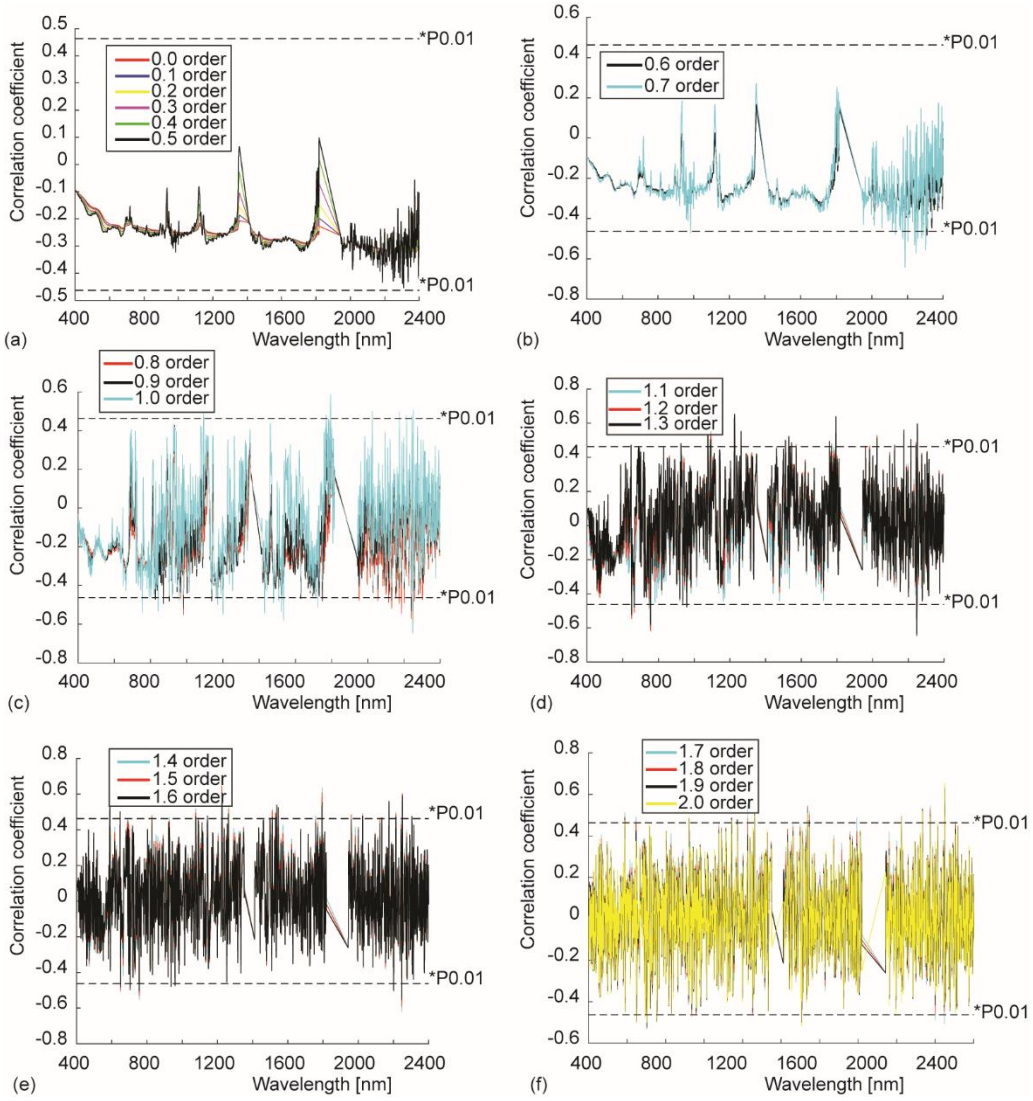

Figure 2. Correlation coefficient between ground temperature and original spectra; (a) 0.0-order to 0.5-order, (b) 0.6-order to 0.7-order, (c) 0.8-order to 1.0-order, (d) 1.1-order to 1.3-order, (e) 1.4-order to 1.6-order, (f) 1.7-order to 2.0-order,

2.0-order is greater than that of 0.5. Table 1 shows that the soil spectrum has a certain correlation with the ground temperature.

Prediction model of ground temperature under different fractional-order derivate

The wavelength bands greater than 0.5 in tab. 1 are selected as feature bands, and a linear model was established by stepwise multiple regression. Eighteen samples are randomly selected to model, and the remaining samples are used to verify the reliability of the prediction model. The simulation results are shown in tab. 2. It can be seen from tab. 2 that the R^2 of 0.7,

0.8, 0.9, 1.3, 1.4, 1.5, 1.6, and 1.7-order is greater than 0.66, indicating that the established model has a better fitting effect. The fitting results are shown in fig. 3.

Table 1. Significance bands number and max correlation coefficient

Order	Significance bands numbers	Max correlation coefficient		Order	Significance bands numbers	Max correlation coefficient	
		Value	Band			Value	Band
0.0	0	0.33499	2396	1.1	25	0.64864	2248
0.1	0	0.34681	2396	1.2	29	0.64619	2248
0.2	0	0.36598	2396	1.3	33	0.65334	1226
0.3	0	0.39391	2396	1.4	29	0.65822	1226
0.4	0	0.42124	2396	1.5	27	0.64387	1226
0.5	0	0.45416	2309	1.6	29	0.60892	1226
0.6	10	0.53663	2186	1.7	24	0.57235	2251
0.7	17	0.64431	2186	1.8	18	0.60005	2250
0.8	16	0.62747	2248	1.9	17	0.63334	2250
0.9	24	0.64456	2248	2.0	17	0.65702	2249
1.0	32	0.64749	2248				

Table 2. Prediction model of ground temperature

Order	Calibration set		Verification set		Order	Calibration set		Verification set	
	R^2	RMSE	R^2	RMSE		R^2	RMSE	R^2	RMSE
0.0	–0.098	6.8476	0.000015	7.5468	1.1	0.629	3.9791	0.5867	7.6345
0.1	0.056	6.3474	0.3511	5.5366	1.2	0.733	3.3780	0.6547	8.0024
0.2	0.083	6.2565	0.4015	5.0573	1.3	0.754	3.2416	0.684	8.1680
0.3	0.363	5.2159	0.5201	6.9298	1.4	0.752	3.2560	0.6955	8.1755
0.4	0.427	4.9448	0.5294	6.4536	1.5	0.727	3.4135	0.6935	8.0795
0.5	0.474	4.7393	0.5642	5.9654	1.6	0.668	3.7643	0.6834	7.8210
0.6	0.519	4.5296	0.6361	5.7706	1.7	0.571	4.2812	0.6736	7.3330
0.7	0.543	4.4158	0.7142	5.9836	1.8	0.452	4.8358	0.6534	6.8502
0.8	0.480	4.7110	0.7323	6.0964	1.9	0.336	5.3245	0.5945	6.6338
0.9	0.300	5.4667	0.6963	5.2006	2.0	0.167	5.9647	0.4391	6.1946
1.0	0.294	5.4901	0.5367	6.1866					

Conclusion

This paper collected the field spectrum of Xinjiang soil and the ground temperature of the sample. The prediction of ground temperature based on soil field spectrum using fractional derivative is studied. The simulation shows that R^2 of 0.7, 0.8, 0.9, 1.3, 1.4, 1.5, 1.6,

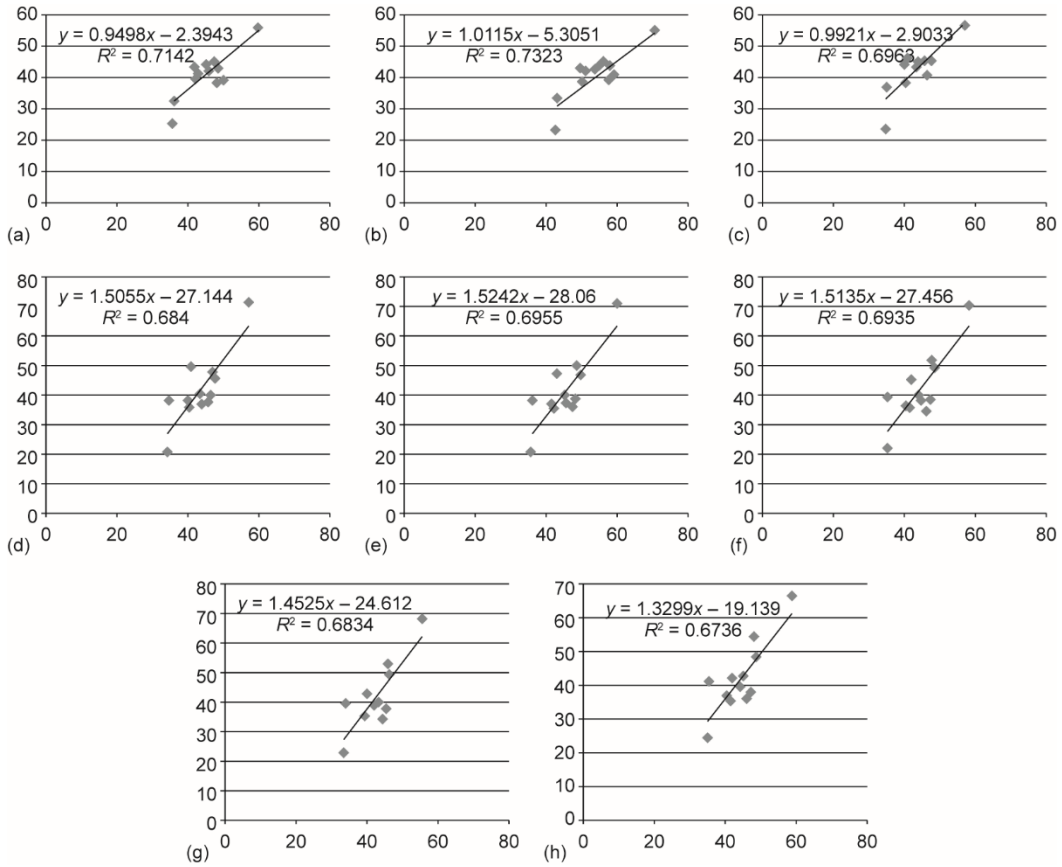

Figure 3. Some fractional order results of prediction model; the horizontal axis is the spectral reflectance value of a sampling point, the vertical axis is the salt value; (a) 0.7-order, (b) 0.8-order, (c) 0.9-order, (d) 1.3-order, (e) 1.4-order, (f) 1.5-order, (g) 1.6-order, (h) 1.7-order

and 1.7-order is greater than 0.66, indicating that the established model has a better fitting effect. It also shows that the soil field spectrum has a certain correlation with the ground temperature, which provides a scientific basis for the quantitative inversion of ground temperature in the future. This paper adopts Gruenwald-Letnikov fractional derivative, other fractional derivatives like He's fractional derivative and fractal derivative [12-26] also work for the present study. Variational principles for fractional calculus becomes a hot topic and can be applied to the present study in future. Wang *et al.* [21] applied the semi-inverse method [27-30] to establish for the first time a variational principle in fractal space, Wang and He [22] suggested a modified Wang's fractal variational principle considering a fractal time, the fractal variational principle provides a good mathematical tool to dynamical prediction of the ground temperature.

Acknowledgment

The authors would like to thank the financial support of National Natural Science Foundation of China (41901065, 41671198, 31660680), Yunnan Province Science and Tech-

nology Department and Education Department Project of China (2017FH001-067, 2017FH001-117), and Research Project of Qujing Normal University (2019JZ001), China.

References

[1] Li, Z. L., *et al.*, Satellite-Derived Land Surface Temperature: Current Status and Perspective, *Remote Sensing of Environment, 131* (2013), Apr., pp. 4-37
[2] Sun, K., *et al.*, Genetic Algorithm Based Surface Component Temperatures Retrieval by Integrating MODIS TIR DATA from Terra and Aqua Satellites, *Journal of Infrared and Millimeter Waves*, *31* (2012), 5, 462-468
[3] Weng, Q. H., *et al.*, A Sub-Pixel Analysis of Urbanization Effect on Land Surface Temperature and Its Interplay with Impervious Surface and Vegetation Coverage in Indianapolis, United States, *International Journal of Applied Earth Observation and Geoinformation*, *10* (2008), 1, pp. 68-83
[4] Fu, P., *et al.*, A Time Series Analysis of Urbanization Induced Land Use and Land Cover Change and Its Impact on Land Surface Temperature with Landsat Imagery, *Remote Sensing of Environment*, *175* (2016), Mar., pp. 205-214
[5] Lu, D. M., *et al.*, The Effect of Urban Expansion on Urban Surface Temperature in Shenyang, China: An Analysis with Landsat Imagery, *Environmental Modeling & Assessment*, *20* (2015), 3, pp. 197-210
[6] Zhong, X. K., *et al.*, Retrieving Land Surface Temperature from Hyperspectral Thermal Infrared Data Using a Multi-Channel Method, *Sensors*, *16* (2016), 5, 687
[7] Zhuo, H. F., *et al.*, Improvement of Land Surface Temperature Simulation over the Tibetan Plateau and the Associated Impact on Circulation in East Asia, *Atmospheric Science Letters*, *17* (2016), 2, pp. 162-168
[8] Liu, K., *et al.*, Analysis of the Urban Heat Island Effect in Shijiazhuang, China Using Satellite and Airborne Data, *Remote Sensing, 74* (2015), 4, pp. 4804-4833
[9] Xia, N., *et al.*, Influence of Fractional Differential on Correlation Coefficient between EC1:5 and Reflectance Spectra of Saline Soil, *Journal of Spectroscopy, 2017* (2017), ID 1236329
[10] Wang, J. Z., *et al.*, Quantitative Estimation of Soil Salinity by Means of Different Modeling Methods and Visible-Near Infrared (VIS-NIR) Spectroscopy, Ebinur Lake Wetland, Northwest China,. *PEERJ, 6* (2018), e4703
[11] Wang, X. P., *et al.*, New Methods for Improving the Remote Sensing Estimation of Soil Organic Matter Content (SOMC) in the Ebinur Lake Wetland National Nature Reserve (ELWNNR) in northwest China, *Remote Sensing of Environment*, *218* (2018), Dec., pp. 104-118
[12] He, J. H., A Simple Approach to One-Dimensional Convection-Diffusion Equation and Its Fractional Modification for E Reaction Arising in Rotating Disk Electrodes, *Journal of Electroanalytical Chemistry*, *854* (2019), Dec., ID 113565
[13] He, J. H., Variational Principle for the Generalized KdV-Burgers Equation with Fractal Derivatives for Shallow Water Waves, *J. Appl. Comput. Mech.*, *6* (2020), 4, pp. 735-740
[14] Wang, Q. L., *et al.,* Fractal Calculus and Its Application to Explanation of Biomechanism of Polar Bear Hairs, *Fractals*, *26* (2018), 6, 1850086
[15] Wang, Q. L., *et al.* Fractal Calculus and Its Application to Explanation of Biomechanism of Polar Bear Hairs, (vol. 26, 1850086,2018), *Fractals, 27* (2019), 5, 1992001
[16] Wang, Y., Deng, Q., Fractal Derivative Model For Tsunami Travelling, *Fractals, 27* (2019), 1, 1950017
[17] He, J. H., A Tutorial Review on Fractal Space Time and Fractional Calculus, *Int. Journal Theor. Phys.*, *53* (2014), 11, pp. 3698-3718
[18] Wang, K. L., Wang, K. J., A Modification of the Reduced Differential Transform Method for Fractional Calculus, *Thermal Science*, *22* (2018), 4, pp. 1871-1875
[19] He, J. H., Ji, F. Y., Two-Scale Mathematics and Fractional Calculus for Thermodynamics, *Thermal Science, 23* (2019), 4, pp. 2131-2133
[20] Ain, Q. T., He, J. H., On Two-Scale Dimension and Its Applications, *Thermal Science, 23* (2019), 3B, pp. 1707-1712
[21] Wang, Y., *et al.* A Variational Formulation for Anisotropic Wave Traveling in a Porous medium, *Fractals, 27* (2019), Jun, 1950047
[22] Wang, K. L., He, C. H., A Remark on Wang's Fractal Variational Principle, *Fractals*, *27* (2019), 8, ID 1950134

[23] Fan, J., *et al.*, Fractal Calculus for Analysis of Wool Fiber: Mathematical Insight of Its Biomechanism, *Journal of Engineered fibers and Fabrics, 14* (2019), 1-4, pp. 1-4
[24] Zhang, J. J., *et al.* Some Analytical Methods for Singular Boundary Value Problem in a Fractal Space, *Appl. Comput. Math., 18* (2019), 3, pp. 225-235
[25] Liu, F. J., *et al.*, A Delayed Fractional Model for Cocoon Heat-Proof Property, *Thermal Science*, *21* (2017), 4, pp. 1867-1871
[26] Liu, H.Y., *et al.*, Fractional Calculus for Nanoscale Flow and Heat Transfer, *International Journal of Numerical Methods for Heat & Fluid Flow, 24* (2014), 6, pp. 1227-1250
[27] Li, Y., He, C. H., A Short Remark on Kalaawy's Variational Principle for Plasma, *International Journal of Numerical Methods for Heat & Fluid Flow, 27* (2017), 10, pp. 2203-2206
[28] He, J. H., A Modified Li-He's Variational Principle for Plasma, *International Journal of Numerical Methods for Heat and Fluid Flow*, On-line first, https://doi.org/10.1108/HFF-06-2019-0523, 2019
[29] He, J. H., Lagrange Crisis and Generalized Variational Principle for 3D Unsteady Flow, *International Journal of Numerical Methods for Heat and Fluid Flow,* On-line first, https://doi.org/10.1108/HFF-07-2019-0577, 2019
[30] He, J. H., Sun, C., A Variational Principle for a Thin Film Equation*, Journal of Mathematical Chemistry, 57* (2019), 9, pp. 2075-2081

Paper submitted: December 16, 2018
Paper revised: June 19, 2019
Paper accepted: August 18, 2019